RAPID COMMUNICATIONS

PHYSICAL REVIEW B VOLUME 45, NUMBER 20 15 MAY 1992-II

Observation of magnetophonon resonance in the miniband transport in semiconductor superlattices

H. Noguchi and H. Sakaki
Institute of Industrial Science, University of Tokyo, 7-22-1 Roppongi, Minato-ku, Tokyo 106, Japan
and Research Center for Advanced Science and Technology, University of Tokyo,
4-6-1 Komaba, Meguro-ku, Tokyo 153, Japan

T. Takamasu and N. Miura
Institute for Solid State Physics, University of Tokyo, 7-22-1 Roppongi, Minato-ku, Tokyo 106, Japan
(Received 25 November 1991; revised manuscript received 12 February 1992)

We have studied vertical transport of electrons in GaAs/$Al_xGa_{1-x}As$ superlattices by applying high magnetic fields normal to the layers. Strong oscillations of magnetophonon resonance are observed in the temperature range between 150 and 300 K, reflecting the singularity of density of states in the superlattice miniband under quantizing magnetic fields. The miniband-width dependence of the resonant spectra is explained by the formation of forbidden gaps between Landau minibands.

Semiconductor superlattices[1] (SLs) provide novel physical phenomena that are not achieved in natural solids. Most of the interesting theoretical features such as Bloch oscillations and the related negative differential conductivity lie in the electron transport through "minibands" obtained by an artificially modulated periodic potential. These theoretical interests have stimulated experimental effort[2-8] on the study of the vertical transport properties of SLs.

In this paper, we report longitudinal magnetoresistance (LMR) in GaAs/$Al_xGa_{1-x}As$ SLs under high magnetic fields normal to the interfaces and parallel to the electronic fields. When electronic motion in the SL layer (xy plane) is quantized by the magnetic field **B**, the electron energy is written as

$$\varepsilon(\mathbf{k}) = \varepsilon_{SL}(k_z) + (n+\tfrac{1}{2})\hbar\omega_c, \quad n=0,1,2,\ldots, \qquad (1)$$

where $\varepsilon_{SL}(k_z)$ is the energy dispersion of the miniband, ω_c is the cyclotron frequency ($=eB/m^*$), and all other symbols have their usual meanings. The dispersion relation and the density of states (DOS) of this system are shown in Fig. 1 for the specific case where the miniband width is 18 meV and the Landau level spacing $\hbar\omega_c$ is 36 meV. When the magnetic field is high enough to make $\hbar\omega_c$ larger than the miniband width, there appear real forbidden gaps where no electronic states are allowed. Note that this magnetic quantization removes many of the complications associated with the lateral motion and gives rise to a simple density of states which is determined by the miniband structure. Hence, the scattering processes are greatly simplified and the SL miniband structure is expected to be clearly reflected in transport properties. Here we studied LMR at high temperatures from 150 to 300 K, and observed large resonant peaks caused by longitudinal magnetophonon resonance (LMPR).[9]

The experimental arrangement is illustrated in the inset in Fig. 2(a). A series of GaAs/$Al_xGa_{1-x}As$ superlattices was grown by molecular-beam epitaxy (MBE) on n^+-type GaAs substrates. The samples consist of 50 periods of the well (thickness L_w) and the barrier (L_B) and are sandwiched by 5000-Å-thick Si-doped GaAs layers with a donor density of about 1×10^{18} cm^{-3}. Since the four-point probe method can hardly be used in the vertical transport measurement, the resistance of SL layer must be set far higher than the Ohmic resistance of n^+ electrodes. Hence, we employed a δ-like doping scheme. Only the 2-4-Å-thick layer at the center of the barriers was doped with Si to about 1×10^{17} cm^{-3}. This scheme reduces the average carrier density $N_{av}=10^{15}$-10^{16} cm^{-3}, which is low enough as compared with that in the highly doped electrode layers. After forming an Ohmic contact with Au-Ge on the surface, the sample was etched to mesa structure with diameter of 100 μm. Listed in Table I are the structures, donor densities N_d, N_{av}, miniband width ε_b, and zero magnetic-field resistance R_0 at 230 K of five samples (A-E). The SL periods listed here are determined from x-ray diffraction, and are close to the sum $L_{SL}=L_w+L_B$ determined from the growth rate. The miniband width is calculated by the Kronig-Penney model.[10] The electron mobility normal to the layers is about 100 cm^2/Vs when estimated from the conductivity and

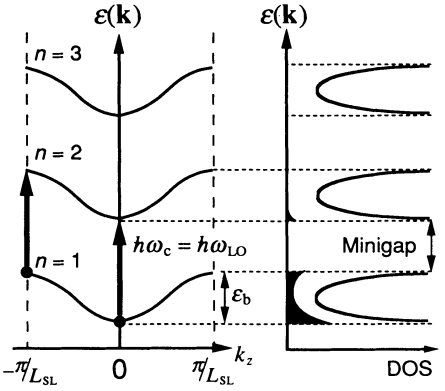

FIG. 1. Dispersion relation and density of states of a superlattice under high magnetic fields and the resonant excitation of electrons by optical phonons. The number n on each miniband is the Landau index. The shaded area in the DOS indicates distributed electrons at high temperatures.

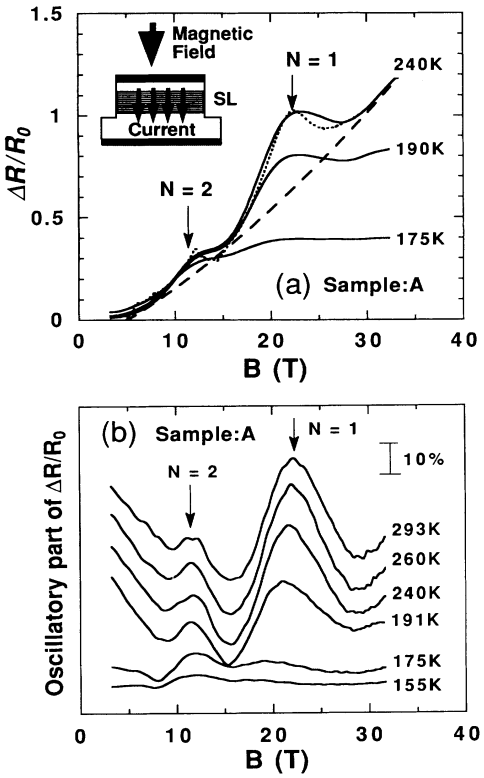

FIG. 2. (a) The longitudinal magnetoresistance ΔR of a superlattice sample A at three temperatures normalized by zero-field resistance R_0. Here, $R_0=25\ \Omega$ ($T=240$ K), 30 Ω (190 K), and 32 Ω (175 K). The dashed line indicates a fitting curve used to subtract the monotonous background from the data at 240 K. The dotted line set on the data at 240 K is calculated for $\varepsilon_b=20$ meV (see the text). Inset: A schematic illustration of the sample structure and experimental setup to measure the longitudinal magnetoresistance of a superlattice. (b) The magnetophonon resonance spectra of sample A after subtracting the background resistance. Each spectrum is shifted vertically for easy comparison. The vertical scale shows the amplitude of ΔR normalized with the zero-field resistance. See the text and Table I for the details of sample A.

the electron concentration. This indicates that electrons in these SL layers flow by miniband transport, and not by hopping.

LMR was measured by applying 5–10-msec pulsed magnetic fields normal to the surface up to 35 T. The typical current level was 100 μA and the applied voltage was less than 4 mV, which is small enough to maintain the Ohmic transport through the ground miniband. The details of this measurement system are described in Ref. 11. Figure 2(a) shows the LMR measured on sample A at various temperatures. The vertical axis of Fig. 2(a) denotes the increase ΔR of LMR normalized by R_0 whose temperature dependence is listed in the figure caption. On top of the increasing background resistance, two large peaks are observed at 12 and 22 T; they correspond approximately to the condition for magnetophonon resonance:[9]

$$N\omega_c(=NeB/m^*)=\omega_{\mathrm{LO}}, \tag{2}$$

with $N=2$ and 1, respectively. Here, ω_{LO} is the optical phonon frequency and m^* is the in-plane effective mass of electrons. As shown in Fig. 1, electrons accommodated in the ground Landau level can be excited to the second (third) Landau level by optical phonon scattering at $N=1$ (2) resonance. Note that the resonant peaks appear at rather high temperatures above 150 K since the LO phonon population increases almost exponentially with temperature.

The background component of magnetoresistance which increases monotonically with magnetic field is most likely caused by phonon scattering because the magnetoconfinement of electrons strengthens in general the electron-phonon interactions in the lateral plane. Since we are concerned here only with peak positions and line shapes of LMPR, we subtract from the data this monotonous background which can be approximated by second-order polynomials as shown by the dashed line in Fig. 2(a). The validity of this subtraction will be discussed in detail later. In Fig. 2(b) LMPR spectra of sample A after the background subtraction are shown with each spectrum shifted vertically for comparison. A remarkable point is that the amplitude of the fundamental peak at $N=1$ resonance exceeds 20% of the zero-field resistance, while the modulation in bulk is less than 5%.[9] This enhancement of the peak intensities in SLs can be explained by the following argument.

Our experiment corresponds to a case of low carrier density (10^{15}–10^{16} cm^{-3}) and high magnetic fields (10–25 T). In this condition, since each Landau miniband can accommodate about 10^{18} cm^{-3} electrons, most of the electrons are distributed in the lowest Landau miniband even at high temperatures as shown in the shaded area in Fig. 1. Then the resistance or the scattering rate

TABLE I. The structural parameters, miniband width ε_b, and zero field resistance R_0 of SL samples used in the experiment. The period of SL is obtained by the measurement of x-ray diffraction. N_d and N_{av} denotes the carrier density of the doping layer and its average including the nondope layer, respectively.

Sample	L_w (Å)/L_B (Å)	SL period	Al content x	N_d (10^{16} cm^{-3})	N_{av} (10^{15} cm^{-3})	ϵ_b (meV)	R_0 (230 K) (Ω)
A	60/30	· · ·	0.29	7.4	1.6	20.2	27
B	50/48	99.3	0.30	10	4.0	8.5	12
C	60/40	100.6	0.31	10	4.0	9.3	9.2
D	60/35	95.6	0.31	10	4.2	12.9	3.1
E	64/27	90.7	0.30	5.0	5.9	21.5	5.6

by optical phonons should be proportional to the product of densities of the initial and the final states. Since all the states must be accommodated in the narrow energy range of the minibands, the DOS of SLs under a high magnetic field usually gets far larger than that of the bulk, especially when the miniband width decreases. As a consequence, the DOS shows distinct peaks at the top and the bottom of minibands; this leads to the enhancement of optical phonon scattering rate when the resonance condition [Eq. (2)] is satisfied. In contrast, when the resonance condition breaks, electron transitions by optical phonons may be inhibited, since final states are not available as discussed later. This explains why the magnetophonon resonance peaks are seen more clearly in SLs than in three-dimensional (3D) bulk. Note also that in SLs we can neglect such complications as pseudoresonance[12] and acoustic-phonon-scattering assisted processes[13] because of the split of minibands.

Next, we discuss the effect of miniband width ε_b on the behavior of MPR around 230 K. We studied four SL samples (B-E) that cover the miniband width ranging from 8 to 20 meV. Figure 3 shows the MPR spectra obtained in the same manner as Fig. 2, while each of the spectra is somewhat enlarged to normalize the $N=1$ peak amplitude. We can easily see that the amplitude of the $N=2$ resonance peak as compared to the $N=1$ peak gets smaller with increasing miniband width. This can be understood by considering the scattering rate; when the miniband is wide ($\sim$20 meV) and the Landau energy $\hbar\omega_c$ is small ($\lesssim$20 meV at 12 T), the minigap shown in Fig. 1 disappears. In such a condition the resonant feature of the scattering rate becomes weak since the DOS of each miniband broadens and overlaps, resulting in the reduction of its peaked feature. Hence, the discrete features of DOS are essential to observe clear resonance peaks.

Note also that the observed width of $N=1$ resonant peaks in Fig. 3 decreases with the miniband width ε_b. When ε_b is smaller than 10 meV, a plateaulike feature appears clearly between the two MPR peaks. This suggests

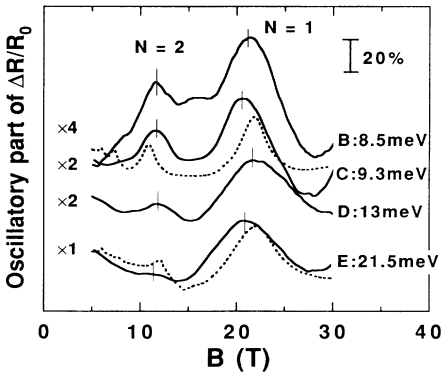

FIG. 3. The magnetophonon resonance spectra of four SL samples (B-E) at around 230 K. Each spectrum is enlarged so that the $N=1$ peak has the same amplitude as the others. The scale (20%) indicates the magnitude relative to the zero-field resistance. The dotted lines set to the samples C and E indicate the calculated results for $\varepsilon_b=10$ and 20 meV, respectively.

that the contribution of the LO phonon is relatively small in this region. This miniband-width dependence of the MPR spectra and the plateau feature can be explained by considering the availability or the disappearance of the final states; electrons in the first Landau miniband can absorb the LO phonon (energy $\hbar\omega_{\mathrm{LO}}$) and reach the energy range between $\hbar\omega_{\mathrm{LO}}$ and $\hbar\omega_{\mathrm{LO}}+\varepsilon_b$. This process is possible only when the energy of such final states falls on the $(n+1)$th Landau miniband. This condition can be expressed as

$$\hbar\omega_{\mathrm{LO}}-\varepsilon_b<n\hbar\omega_c<\hbar\omega_{\mathrm{LO}}+\varepsilon_b \tag{3}$$

for the $(n+1)$th miniband, which corresponds to the nth MPR peak. Therefore, the width of MPR peak should be mainly determined by the miniband width when the peaks do not overlap each other.

If a SL with sufficiently narrow miniband is placed in high magnetic fields ($\hbar\omega_c=\hbar eB/m^*>\varepsilon_b$), the real minigap will be formed between the adjacent minibands. Particularly when the condition

$$(\hbar\omega_{\mathrm{LO}}+\varepsilon_b)/2<\hbar\omega_c<\hbar\omega_{\mathrm{LO}}-\varepsilon_b \tag{4}$$

is satisfied, final states are completely inside the minigap. In other words, we are in a novel case where the magnetic field is too small to cause the $N=1$ resonance and yet too large to achieve the $N=2$ resonance. Hence the optical phonons cannot excite electrons to higher-lying states. For example, when $\varepsilon_b=8$ meV the case defined by Eq. (4) corresponds to $12.8<B<16.3$ T. This explains why the plateau appears between the two peaks. Thus the optical phonon scattering in this region is effectively inhibited. This situation is quite similar to the case of coupled quantum box structures which was proposed earlier by Sakaki[14] as a novel scheme to suppress the optical phonon scattering in semiconductors.

To examine the above argument more quantitatively, we perform a simple calculation using Eqs. (6)-(9) of Ref. 15 and evaluate the resistivity component $\rho_{\mathrm{opt}}(B)$ which is dominated by the optical phonon scattering.[16] Here, we use $\hbar\omega_{\mathrm{LO}}=36$ meV and $m^*=0.067$. The total resistivity $\rho_{\mathrm{tot}}(B)$ can then be expressed as

$$\rho_{\mathrm{tot}}(B)=\rho_{\mathrm{opt}}(B)+C_1B+C_0. \tag{5}$$

The linear term C_1B represents the scattering process by acoustic phonons at high magnetic fields since it increases inversely proportional to the square of the cyclotron radius.[17] By choosing the parameters C_0 and C_1, we obtained a theoretical line [a dotted line in Fig. 2(a)] which reproduces the experimental result fairly well.

The same analysis was carried out for the samples C and E, and we obtained again good agreements between experiments and theory. Then, to clarify the detail of the spectrum, we subtracted the background component from both theory and data by using the same function. The calculated spectra after this subtraction are shown by the dotted lines in Fig. 3. They reproduce quite well the features of experimental data including the plateau region in spite of their simplicity. Note that the plateau on the theoretical line completely corresponds to the region described by Eq. (4). Therefore, the magnetoresistance in

this plateau region should be determined mainly by acoustic-phonon scattering which leads to the monotonous increase of the resistance. Thus, the appearance of the plateau indicates the existence of the real band gap between Landau minibands.

Figure 3 shows that the measured peak position at $N=1$ is lower than that calculated by using the bulk phonon energy and effective mass. This discrepancy may be ascribed to the sophistication of phonon energies confined in the SL layers.[18] This point needs further investigation.

In summary, we have investigated the vertical transport in semiconductor superlattices by applying high magnetic fields up to 35 T normal to the layers. The magnetophonon resonance far larger than that in bulk has been observed. This enhancement of the resonant peaks is found to result from the formation of narrow minibands and the real minigaps between them. When the miniband is sufficiently narrow, a plateau appears between two resonant peaks and is found to correspond to the region where the optical phonon scattering is inhibited.

We would like to thank S. Koshiba for the x-ray measurement. This work is partly supported by a Grant-in-Aid for Scientific Research from the Ministry of Education, Science and Culture and also partly by the JRDC through the ERATO project on quantum wave.

[1]L. Esaki and R. Tsu, IBM J. Res. Dev. **14**, 61 (1970).
[2]B. Deveaud, J. Shah, T. C. Damen, B. Lambert, and A. Regreny, Phys. Rev. Lett. **24**, 2582 (1987).
[3]T. Duffield, R. Bhat, M. Koza, F. DeRosa, K. M. Rush, and S. J. Allen, Jr., Phys. Rev. Lett. **59**, 2693 (1987).
[4]E. E. Mendez, F. Agullo-Rueda, and J. M. Hong, Phys. Rev. Lett. **60**, 2426 (1988).
[5]M. Helm, P. England, E. Colas, F. DeRosa, and S. J. Allen, Jr., Phys. Rev. Lett. **63**, 74 (1989).
[6]A. Sibille, J. F. Palmier, H. Wang, and F. Mollot, Phys. Rev. Lett. **64**, 52 (1990).
[7]B. J. Skromme, R. Bhat, M. A. Koza, S. A. Schwarz, T. S. Ravi, and D. M. Hwang, Phys. Rev. Lett. **65**, 2050 (1990).
[8]P. England, J. R. Hayes, E. Colas, and M. Helm, Phys. Rev. Lett. **63**, 1708 (1989).
[9]For reviews, see R.J. Nicholas, Prog. Quantum Electron. **10**, 1 (1985); R. A. Stradling and R. A. Wood, J. Phys. C **1**, 1711 (1968).
[10]G. Bastard, Phys. Rev. B **24**, 5693 (1981).
[11]G. Kido, N. Miura, H. Ohno, and H. Sakaki, J. Phys. Soc. Jpn. **51**, 2168 (1982).
[12]R. L. Peterson, Phys. Rev. B **6**, 3756 (1972).
[13]V. L. Gurevich and Y. A. Firsov, Zh. Eksp. Teor. Fiz. **47**, 734 (1964) [Sov. Phys. JETP **20**, 489 (1965)].
[14]H. Sakaki, Jpn. J. Appl. Phys. **28**, L361 (1989).
[15]V. M. Polyanovskii, Fiz. Tekh. Poluprovodn. **17**, 1801 [Sov. Phys. Semicond. **17**, 1150 (1983)].
[16]H. Noguchi, T. Takamasu, N. Miura, and H. Sakaki, Surf. Sci. (to be published).
[17]S. Briggs and J. P. Leburton, Phys. Rev. B **38**, 8163 (1988).
[18]G. Fasol, M. Tanaka, H. Sakaki, and Y. Horikoshi, Phys. Rev. B **38**, 6056 (1988).